

See discussions, stats, and author profiles for this publication at: <https://www.researchgate.net/publication/376190766>

# Line Fitting-Based Corner-Like Detector for 2D Laser Scanners Data

Preprint · November 2023

DOI: 10.13140/RG.2.2.11269.32480

CITATIONS

0

READS

274

4 authors:



**Ricardo B. Sousa**

Institute for Systems and Computer Engineering, Technology and Science (INESC TEC)

43 PUBLICATIONS 168 CITATIONS

SEE PROFILE



**Heber Sobreira**

Institute for Systems and Computer Engineering, Technology and Science (INESC TEC)

66 PUBLICATIONS 555 CITATIONS

SEE PROFILE



**Manuel F. Silva**

School of Engineering of the Polytechnic Institute of Porto

380 PUBLICATIONS 3,294 CITATIONS

SEE PROFILE







**A. Paulo Moreira**

University of Porto

332 PUBLICATIONS 4,716 CITATIONS

SEE PROFILE

# Line Fitting-Based Corner-Like Detector for 2D Laser Scanners Data\*

Ricardo B. Sousa\* , Héber Miguel Sobreira† , Manuel F. Silva‡  and António Paulo Moreira§ 

\*§Faculty of Engineering, University of Porto, 4200-465 Porto, Portugal

Email: up201503004@edu.fe.up.pt, amoreira@fe.up.pt

\*†‡§INESC TEC – Institute for Systems and Computer Engineering, Technology and Science, 4200-465 Porto, Portugal

Email: heber.m.sobreira@inesctec.pt

‡ISEP, Polytechnic of Porto, R. Dr. António Bernardino de Almeida, 4249-015 Porto, Portugal

Email: mss@isep.ipp.pt

**Abstract**—The extraction of geometric information from the environment may be of interest to localisation and mapping algorithms. Existent literature on extracting geometric features from 2D laser data focuses mainly on detecting lines. Regarding corners, most methodologies use the intersection of line segment features. This paper presents a feature extraction algorithm for corner-like points in the 2D laser scan. The proposed methodology defines arrival and departure neighbourhoods around each scan point and performs local line fitting evaluated in multiple distance-based scales. Then, a set of indicators based on line fitting error, the angle between arrival and departure lines, and consecutive observation of the same keypoint across different scales determine the existence of a corner-like feature. The experiments evaluated the corner-like features regarding their relative position and observability, achieving standard deviations on the relative position lower than the sensor noise and visibility ratios higher than 75% with very low false positives rates.

**Index Terms**—corner detector, feature extraction, 2D laser scanner, localisation, mobile robots

## I. INTRODUCTION

In recent years, autonomous mobile robots have become increasingly employed in a wide range of applications, from manufacturing and logistics to healthcare and home automation. One of the key challenges in developing effective mobile robot navigation systems is accurately localising the robot within its surroundings [1]. The pose may be obtained by comparing the current observation of the onboard sensors to the robot's current knowledge of the environment [2].

Typical sensors used on industrial and service mobile robots are 2D laser scanners coupled with wheeled odometry, given that the corresponding applications usually only require 2D localisation. Laser scanners allow to build a dense representation of the environment as a 2D occupancy grid map, where each cell represents occupied, free, or unknown space [3]. Although grid maps can represent arbitrary objects, they are computationally expensive and require a huge amount of memory [4]. An alternative method is to represent the environment with features. In the case of 2D lasers, the features may be

beacons [5], geometric cues – line [6–14] and curve [10–12, 15] segments, corners [6–12, 15–19], and edges (free endpoint of segments) [6, 11, 16, 19] –, or semantic features such as parked vehicles [17, 20] and doors [7].

The physical correspondence of geometric features to the environment (e.g., lines and corners) may be of interest for the localisation and mapping problems on mobile robots, but also to interact with the user of autonomous mobile systems. The current literature presents several algorithms to extract line segments from 2D laser scan data [6–14], including an open-source implementation based on the Robot Operating System (ROS) framework<sup>1</sup>. As for corner detection, the most common methodology found in the literature is to extract corners from the intersection of line segments detected in the laser scan [6–9, 15, 17–22]. However, this methodology makes the corner detection highly dependent on the line detection algorithm and possibly limited to well-structured environments. Another approach found in the literature is to estimate the curvature on the scan data [10–12, 16]. Still, the influence of the sensor noise in the curvature estimation may lead to variant features and false positives.

Given these limitations, this paper presents a feature extraction algorithm to detect points of interest in 2D laser scan data that resemble a physical corner. The proposed algorithm performs local line fitting evaluated in multiple distance-based scales around a certain point, similar to Speeded Up Robust Features (SURF) [23]. These scales define arrival and departure neighbourhoods around the points in the scan. The intersection of the fitted lines defines candidate feature keypoints. Then, a set of indicators based on line fitting error, angle between the arrival and departure lines, and consecutive observation of the same candidate keypoint across different scales determine the definition of a corner-like feature. The proposed methodology is independent of global search in the scan for line segments, allowing other feature extraction methods to be executed concurrently. Also, the experimental results show that the perceived keypoints are not only structure corners but also other points of interest in the environment. This result indicates that the proposed extractor algorithm is

This work is co-financed by Component 5 – Capitalisation and Business Innovation, integrated in the Resilience Dimension of the Recovery and Resilience Plan within the scope of the Recovery and Resilience Mechanism (MRR) of the European Union (EU), framed in the Next Generation EU, for the period 2021–2026, within project GreenAuto, with reference 54.

<sup>1</sup>[https://github.com/kam3k/laser\\_line\\_extraction](https://github.com/kam3k/laser_line_extraction)

not limited to well-structured environments. Finally, an open-source implementation compatible with the ROS framework is available in a GitHub repository<sup>2</sup>.

The rest of the paper is organised as follows. Section II presents an analysis on methods found in the literature for corner detection. Next, Section III formulates the proposed corner-like feature extraction algorithm on 2D laser data. Section IV analyses the results obtained from the experiments made. Lastly, Section V presents the conclusions of this work.

## II. RELATED WORKS

### A. Line fitting intersection

A trend found in the literature is to extract corners from the intersection of line segments detected in the 2D laser scan [6–9, 15, 17–22]. First, the laser data may be filtered to remove invalid values (zero range values [17]) and possible noise (e.g., considering the minimum distance to the two neighbours of a certain point to remove isolated data [17], mean average filtering [19], or bilateral filters to remove non-linear noise [9]). Next, a segmentation step extracts sets of continuous points in the environment for line fitting estimation. Castellanos et al. [6] segment the scan into polygonal lines and perform subsequent division into segments by an iterative method [24]. Falomir et al. [15] search for discontinuities in the data to form subsets of points and use the recursive line fitting algorithm [25] to obtain the line segments. Fernández-Moral et al. [21] search for parameters of a 2D line that maximise the number of points supporting the lines model using Random Sample Consensus (RANSAC) [26]. Mohamed et al. [8] use the Line Tracking (LT) algorithm [27] to iteratively segment lines in the scan and perform Principle Component Analysis (PCA) to compute the lines' parameters. Then, the intersection points between consecutive line segments define a corner feature in the environment.

Furthermore, Lin et al. [18] and Liu et al. [9, 19] use adaptive threshold segmentation to cluster the range data in subsets of continuous points in space. Although Lin et al. [18] state the use of an adaptive segmentation due to the non-uniform distribution of the 2D laser data, the authors do not specify the threshold used in their work. In Liu et al. [19] method, the threshold is based on the angular resolution of the laser and the distance value of the current point under analysis. Liu et al. [9] establish also a threshold depending on the angular resolution. Instead of only considering the distance of the point under analysis, the proposed approach selects the larger distance measurement in adjacent points. Even though Roumeliotis and Bekey [7] do not use a specific adaptive threshold, the proposed SEGMENTS algorithm with a two-level Extended Kalman Filters (EKF) has an adaptive characteristic. A stricter filter in terms of the system's noise covariance attempts to follow a straight line, while a more flexible EKF tries to follow a new segment when processing

a scan. The four methods [7, 9, 18, 19] also define a corner feature as the intersection between consecutive line segments.

A specific application of corner detection with 2D laser data in the literature is vehicle detection [17, 20]. Jung et al. [17] cluster the laser data based on a fixed threshold between consecutive range values. Then, the method performs template matching to every point under analysis, assuming the point is the vertex of the L-shape of a vehicle in the scan. Jung et al. [17] use Singular Value Decomposition (SVD) to estimate the lines' parameters of the L-shape and decompose the problem in line-curve estimation when the vehicle has a curved corner in the data. In contrast, Qu et al. [20] segment the data using the Density Based Spatial Clustering of Applications with Noise (DBSCAN) [28]. The method performs L-shape fitting in two steps – search for the vertexes of the L-shape and corner point localisation – based on RANSAC [26].

However, corner detection algorithms dependent on global search in the scan for line segments are possibly limited to well-structured environments. Thus, this paper proposes a corner-like detection with local line fitting, not requiring global detection for lines neither recursive search in the data. Also, the experiments presented in Section IV demonstrate the ability of the proposed detector to extract more points of interest from the scan in addition to environment corners.

### B. Curvature-based detection

Other approaches to detect corners in 2D laser data are based on estimating the curvature associated to the scan. Núñez et al. [10] propose an adaptive curvature estimator comparing the  $k$ -nearest points at both sides of the one being evaluated. The  $k$  size is changed according to the distance between possible corners. A segmentation step precedes the curvature estimation to detect breakpoints using the adaptive breakpoint detector proposed by Borges and Aldon [29]. Then, Núñez et al. [10] extract corners, lines, and curve segment features from the scan data by analysing if there are peaks in curvature, flat segments with curvature where the average value is equal to zero, and flat ones with an average curvature different than zero, respectively. Vázquez-Martín et al. [11] use the adaptive curvature estimator of Núñez et al. [10] to segment the scan into clusters of homogeneous curvature. Even though the corner existence is determined from the curvature function, its keypoint definition is based on the intersection of the two line features that generate the corner to improve noise robustness. Also, Certad et al. [16] modify the work of Núñez et al. [10] to consider two curvature estimations from two different noise-related thresholds, improving the rate of true detection for corner and edge features in the experiments.

Moreover, Feng et al. [12] and Zhao et al. [22] state a correlation between the angle difference of two fitted lines around both sides of a scan point to the curvature value. Feng et al. [12] introduce the micro-tangent line function as the variance between two consecutive tangents which belong to two consecutive points in the scan. Similarly to Núñez et al. [10], line and curve segments are extracted from consecutive range readings with variance close to zero and

<sup>2</sup>[https://gitlab.inesctec.pt/mrtdt/open-source/inesctec\\_mrdt\\_line\\_fit\\_based\\_corner\\_detector\\_2d\\_laser](https://gitlab.inesctec.pt/mrtdt/open-source/inesctec_mrdt_line_fit_based_corner_detector_2d_laser)

constant value larger than a threshold, respectively, and corner features from peaks on the variance function. Instead of only considering two consecutive points, Zhao et al. [22] define two distance-based regions on both sides of a point to estimate direction vectors and, consequently, the angle difference between those vectors. Candidate corner points are selected based on a fixed threshold for the angle difference. Then, the corner point is estimated via non-minimal suppression.

Still, most of the curvature-based methods for corner feature extraction associate the keypoint to a laser reading. Given the discrete and radial nature of 2D laser data, the estimated corner may be variant at greater distances. Also, there is the question if the curvature estimators are invariant to scale, angular resolutions, and different points of view. This paper proposes a detector based on the stability of intersection points from the fitted lines at different distance-based scales. Also, the experiments presented in Section IV focus on evaluating the invariance of the extracted corner-like features.

### III. CORNER-LIKE FEATURE DETECTOR

#### A. Linear least-squares regression

A generic definition for the 2D line model is presented in Equation 1, where  $(x, y)$  are the 2D point coordinates and  $\gamma_0$ ,  $\gamma_1$ , and  $\gamma_2$  are the model parameters. However, the solution for the generic definition estimated with a linear least-squares formulation from a set of 2D points would be a null vector.

$$\gamma_0 + \gamma_1 x + \gamma_2 y = 0 \quad (1)$$

An alternative formulation is to characterise the 2D line relative to one of the point coordinates, reducing from three to two parameters in the model. The 2D line formulation illustrated in Equation 2 is relative to the  $y$  coordinate with respect to  $x$ , where  $\beta_1$  is the line slope and  $\beta_0$  is the line intersection on the  $y$ -axis. The least-squares solution for the parameters  $\beta_1$  and  $\beta_0$  from a set of points  $(x_i, y_i), i = 1, \dots, N$  is formulated in Equations 3 and 4, where  $(\bar{x}, \bar{y})$  is the centroid point of the data [30]. Still, this model would not be valid when  $\sum_{i=1}^n (x_i - \bar{x})^2 = 0$ , given the indeterminate form caused in the parameter  $\hat{\beta}_1$  (e.g., all the data points with the same  $x$  coordinate and different  $y$  values).

$$y = \beta_0 + \beta_1 x \quad (2)$$

$$\hat{\beta}_1 = \frac{\sum_{i=1}^n (x_i - \bar{x})(y_i - \bar{y})}{\sum_{i=1}^n (x_i - \bar{x})^2} \quad (3)$$

$$\hat{\beta}_0 = \bar{y} - \hat{\beta}_1 \bar{x} \quad (4)$$

The 2D line can be defined relative to  $x$  with respect to the  $y$  coordinate, as formulated in Equation 5. The parameters of this model are the line slope ( $\alpha_1$ ) and the line intersection on the  $x$ -axis ( $\alpha_0$ ). Nevertheless, this model has also a undetermined form when  $\sum_{i=1}^n (y_i - \bar{y})^2 = 0$  (e.g., all the data points with the same  $y$  coordinate and different  $x$  values).

$$x = \alpha_0 + \alpha_1 y \quad (5)$$

$$\hat{\alpha}_1 = \frac{\sum_{i=1}^n (x_i - \bar{x})(y_i - \bar{y})}{\sum_{i=1}^n (y_i - \bar{y})^2} \quad (6)$$

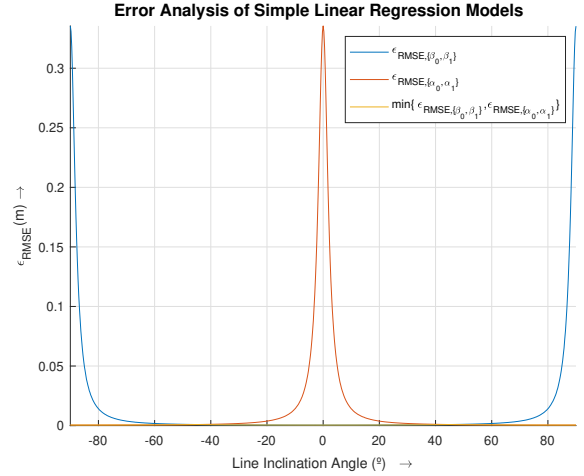


Fig. 1: Error analysis of simple line regression models evaluating the fitting Root-Mean-Square Error (RMSE),  $\varepsilon_{RMSE}$ , for lines with an inclination angle between  $-90^\circ$  and  $90^\circ$  and a simulation step of  $0.25^\circ$ , a set of 100 data points equally distributed along each line, a distance Gaussian noise added to the data point coordinates of zero mean and 0.03 m standard deviation, and 1000 simulation samples per line.

$$\hat{\alpha}_0 = \bar{x} - \hat{\alpha}_1 \bar{y} \quad (7)$$

Instead of only considering a single line model for data fitting, the proposed methodology selects the best line model that fits the laser data. This selection is based on which model has the lower fitting Root-Mean-Square Error (RMSE),  $\varepsilon_{RMSE}$ . Equations 8 and 9 represent the fitting RMSE of the 2D line models formulated in Equations 2 and 5, respectively. The validation of the proposed selection approach for the line models is shown in Figure 1, where selecting the model with the lowest RMSE achieves the best fitting line estimation.

$$\varepsilon_{RMSE, \{\hat{\beta}_0, \hat{\beta}_1\}} = \sqrt{\frac{1}{n} \sum_{i=1}^n (y_i - \hat{\beta}_0 - \hat{\beta}_1 x_i)^2} \quad (8)$$

$$\varepsilon_{RMSE, \{\hat{\alpha}_0, \hat{\alpha}_1\}} = \sqrt{\frac{1}{n} \sum_{i=1}^n (x_i - \hat{\alpha}_0 - \hat{\alpha}_1 y_i)^2} \quad (9)$$

Other models and fitting algorithms could have been considered to fit a line to the 2D laser data, such as formulating a line as the vector to the normal of the infinite line and the position of the weighted mean of the contributing points [13], or using RANSAC to estimate the line parameters of the generic line model [26]. However, these models and fitting algorithms may require iterative-based optimisation procedures and matrices inversions. In contrast, the proposed methodology has the advantage of having closed-form equations for both the line parameters and the fitting error.

#### B. Feature extraction

In terms of extracting features from 2D laser data, first, it is required to transform the scan data from polar to cartesian coordinates. This transformation preserves the order of the data by its angular coordinate to speed up the search for the closest

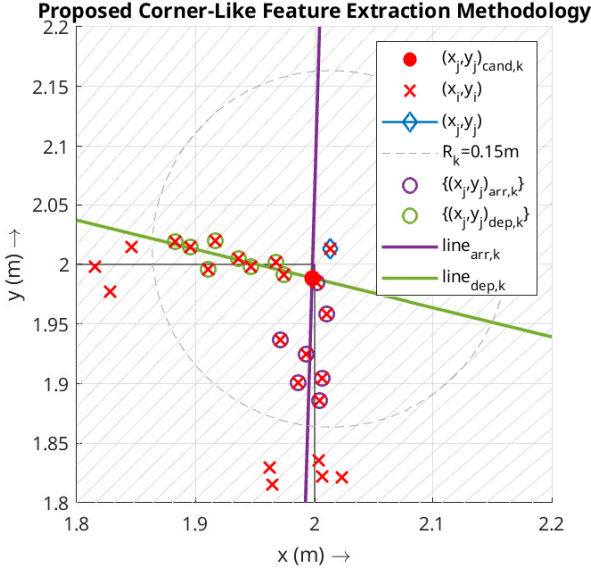


Fig. 2: Example of the proposed corner-like feature extraction methodology on a laser point  $(x_j, y_j)$  at a distance scale  $R_k = 0.15$  m. Scan points  $(x, y)$  simulated considering a 2D laser scanner with  $0.25^\circ$  angular resolution,  $0.06$ – $10.0$  m range, and Gaussian noise with zero mean and  $0.03$  m standard deviation (same specifications as the Hokuyo UST-10LX sensor).

consecutive laser points in the angular direction at a given distance-based neighbourhood.

Next, the proposed feature extraction methodology evaluates each of the laser points  $(x_i, y_i), i = 1, \dots, N$  as a possible feature keypoint. Figure 2 presents an example of the clustering and line fitting results following the proposed methodology on a laser point  $(x_j, y_j)$  at a distance scale  $R_k = 0.15$  m, where this scale defines the distance-based neighbourhood around the scan point. These results illustrate the clustering of the arrival  $((x_i, y_i) \in \{(x_j, y_j)_{arr,k}\})$  and departure  $((x_i, y_i) \in \{(x_j, y_j)_{dep,k}\})$  neighbourhoods, representing the closest consecutive laser points at the negative and positive sides of the point  $(x_j, y_j)$  in the laser angular direction, respectively. The intersection point between the fitted lines  $line_{arr,k}$  and  $line_{dep,k}$  is considered a candidature feature keypoint  $((x_j, y_j)_{cand,k})$ . This intersection point is the result of the lines intersection depending on which line model

$$\begin{aligned} \bullet \quad y &= \beta_0^{arr,k} + \beta_1^{arr,k} x ; y = \beta_0^{dep,k} + \beta_1^{dep,k} x \\ &\begin{cases} x_{j,cand,k} = (\hat{\beta}_0^{dep,k} - \hat{\beta}_0^{arr,k}) / (\hat{\beta}_1^{arr,k} - \hat{\beta}_1^{dep,k}) \\ y_{j,cand,k} = \hat{\beta}_0^{arr,k} + \hat{\beta}_1^{arr,k} \cdot x_{j,cand,k} \end{cases} \end{aligned} \quad (10)$$

$$\begin{aligned} \bullet \quad x &= \alpha_0^{arr,k} + \alpha_1^{arr,k} y ; y = \beta_0^{dep,k} + \beta_1^{dep,k} x \\ &\begin{cases} y_{j,cand,k} = (\hat{\alpha}_0^{arr,k} \hat{\beta}_1^{dep,k} + \hat{\beta}_0^{dep,k}) / (1 - \hat{\alpha}_1^{arr,k} \hat{\beta}_1^{dep,k}) \\ x_{j,cand,k} = \hat{\alpha}_0^{arr,k} + \hat{\alpha}_1^{arr,k} \cdot y_{j,cand,k} \end{cases} \end{aligned} \quad (11)$$

$$\begin{aligned} \bullet \quad y &= \beta_0^{arr,k} + \beta_1^{arr,k} x ; x = \alpha_0^{dep,k} + \alpha_1^{dep,k} y \\ &\begin{cases} y_{j,cand,k} = (\hat{\alpha}_0^{dep,k} \hat{\beta}_1^{arr,k} + \hat{\beta}_0^{arr,k}) / (1 - \hat{\alpha}_1^{dep,k} \hat{\beta}_1^{arr,k}) \\ x_{j,cand,k} = \hat{\alpha}_0^{dep,k} + \hat{\alpha}_1^{dep,k} \cdot y_{j,cand,k} \end{cases} \end{aligned} \quad (12)$$

$$\bullet \quad x = \alpha_0^{arr,k} + \alpha_1^{arr,k} y ; x = \alpha_0^{dep,k} + \alpha_1^{dep,k} y$$

$$\begin{cases} y_{j,cand,k} = (\hat{\alpha}_0^{dep,k} - \hat{\alpha}_0^{arr,k}) / (\hat{\alpha}_1^{arr,k} - \hat{\alpha}_1^{dep,k}) \\ x_{j,cand,k} = \hat{\alpha}_0^{arr,k} + \hat{\alpha}_1^{arr,k} \cdot y_{j,cand,k} \end{cases} \quad (13)$$

The following indicators are evaluated to determine if a candidate keypoint is a corner-like feature or not: minimum of 5 points in each neighbourhood, an absolute angle between arrival and departure fitted lines in the range of  $[45^\circ, 135^\circ]$ , maximum  $\varepsilon_{RMSE}$  in line fitting of  $0.025$  m, maximum distance of the lines intersection points on the multiple scales to the intersection centroid of  $0.025$  m, and maximum distance of the intersection point to the scan point being evaluated of  $0.05$  m. The latter indicator avoids having features not representing physical points. Then, the candidate keypoint is validated if the point passes all previous indicators in a minimum number of 3 consecutive scales, to improve robustness to noise on the laser data. The scales considered in the experiments presented in this paper are the following ones:  $[0.05, 0.075, 0.1, 0.125, 0.15, 0.175, 0.2, 0.225, 0.25]$  m. However, the indicators' thresholds and the scale may be parameterised in run-time. The feature keypoint definition is the lines intersection centroid on the multiple scales.

#### IV. EXPERIMENTAL RESULTS

The experiments were performed using a three-wheeled omnidirectional robot developed by the 5dpo robotics team<sup>3</sup>. This platform was adapted to have a 2D laser scanner, namely, the Hokuyo UST-10LX with  $270^\circ$  Field-Of-View (FOV),  $0.25^\circ$  angular resolution, and  $40$  Hz sampling rate. The sensor is aligned with the geometric centre of the robot, and the wheel odometry parameters were estimated using the OptiOdom [31] calibration method. The implementation of the feature extraction algorithm is in C++ and ROS. The algorithm ran on a computer with a processor Intel Core i7-6700HQ with  $8$  GB of RAM, and a Nvidia GPU GeForce GTX 960M.

In terms of the experimental methodology, first, a map of the scene was retrieved using the Simultaneous Localisation And Mapping (SLAM) Toolbox [32] algorithm with a resolution of  $0.03$  m. Although this algorithm already estimates the robot pose relative to the map being created, this estimation may be improved if the whole map is used to localise the robot. So, the Adaptive Monte Carlo Localisation (AMCL) [33] algorithm available in ROS was used to estimate the robot's localisation relative to the map obtained from the SLAM process. With this localisation estimation, the point clouds from the 2D laser scanner can be transformed to the map coordinate frame that is a static one, instead of being referenced to the moving laser frame. All parameters of the algorithms, launch configuration files, and scripts used in the experiments are also available in this paper's public GitHub repository<sup>2</sup>.

##### A. Feature extraction results

Figure 3 is an example of the feature extraction results. This example represents the extracted features  $(x, y)^{t=t_i}$  at a certain time instant  $t_i$ , where the blue circle is the robot pose estimated by the AMCL [33] algorithm and the orange dotted

<sup>3</sup><https://5dpo.github.io/>



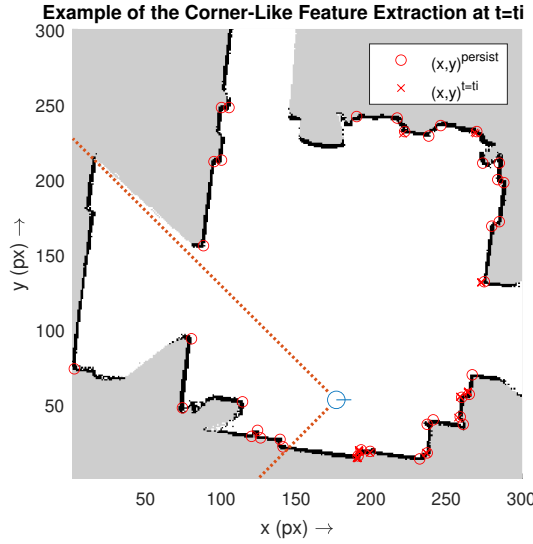


Fig. 3: Example results for the proposed corner-like feature extraction methodology. Occupancy grid map obtained by using the SLAM Toolbox [32] algorithm, considering a map resolution of 0.03 m/px.

lines represent the FOV of the sensor. The points  $(x, y)^{persist}$  represent the locations of the 39 most persistent features in space extracted by the proposed methodology. These locations were found through manual selection of the features location considering their observability through the experiment (see Section IV-B). Further results relative to the features extraction with the proposed methodology are available in videos<sup>4</sup>.

When analysing visually the example results, the persistent features correspond not only to well-defined 90° corners but also to other corner-like points of interest. This observation is shown both in Figure 3 and in the videos<sup>4</sup>, even detecting stable features in legs of passing people through the environment. As for the difference between the features detection at a certain time instant and the most persistent ones, this different may be due to noise in the distance measures of the 2D laser.

### B. Features observability

Next, the observability of the features extracted when moving the robot through the scene shown in Figure 3 was evaluated by processing the features location in the global map frame, using the experimental methodology explained previously. Figure 4 represents a colour map of the features observability ratio, considering the FOV of the sensor and the robot pose throughout time. This colour map considers the same resolution of 0.03 m/px as the one used to localise the robot. Also, the observability map allowed the manual selection of the 39 persistent features also shown in Figure 3.

The first observation is the lower number of false positives. Other than the locations near the 39 most persistent features, the observability ratio of the other areas of the map is lower than 1.0%. Furthermore, there is a blur in the observability ratio near the location of the 39 persistent features, instead

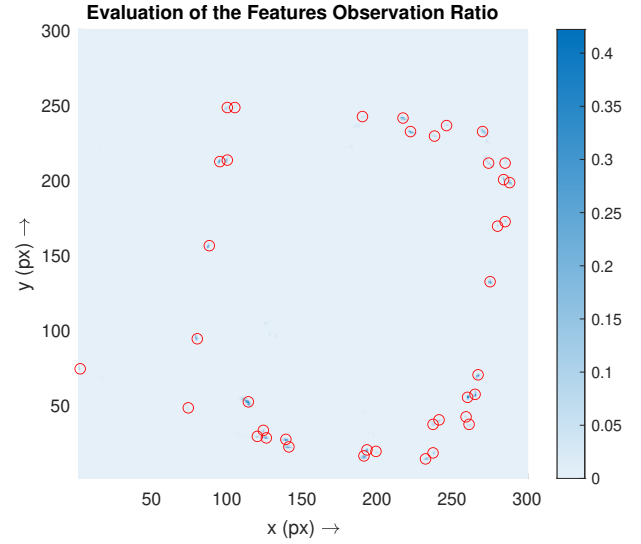


Fig. 4: Evaluation of the features observation ratio, considering the robot pose along time, the Field-Of-View (FOV) of the 2D laser scanner, and a map resolution of 0.03 m/px.

of being concentrated in a single pixel. This blur is a consequence of the uncertainty of the location estimation of the robot, explaining why the maximum observability ratio when considering the resolution of 0.03 m/px of the map was only 42.23%. Indeed, if the observability analysis considers the N8-neighbourhood of each pixel, this maximum observability ratio increases to 100% for 6 features. For the same consideration of the N8-neighbourhood, 20 and 16 features have an observability ratio greater or equal to 50% and 75%, respectively. These results indicate the possible usefulness of the proposed corner-like feature detector for tasks such as localisation and mapping using 2D lasers.

### C. Features association distance

Even though the analysis on the features observability indicate if the features are consistently seen in space, this evaluation is highly dependent on the location estimator required to transform the point cloud to a static frame. Another possible analysis in the context of feature-based localisation systems is to evaluate the distance between different features throughout time, assessing their relative position instead of the absolute one in space. So, Figure 5 presents the analysis on the feature association distance in terms of standard deviation to evaluate the uncertainty on the relative position between the 39 most persistent features selected previously (see Figure 4). The estimation of the standard deviation only considers valid contributing measures, i.e., only consider the distance between two features if both are visible in the same time instant. This estimation was possible by associating the features observable in each time instant to one of the 39 persistent ones if the error distance to the location manually selected is lower than 0.06 m. The latter threshold was needed to account both the unknown uncertainty of the location estimator and the noise on the laser

<sup>4</sup><https://www.youtube.com/watch?v=desB9LX4hck&list=PLvp8fJUEPxYQjsuJAeiBVLEKuBU4Otu7e>

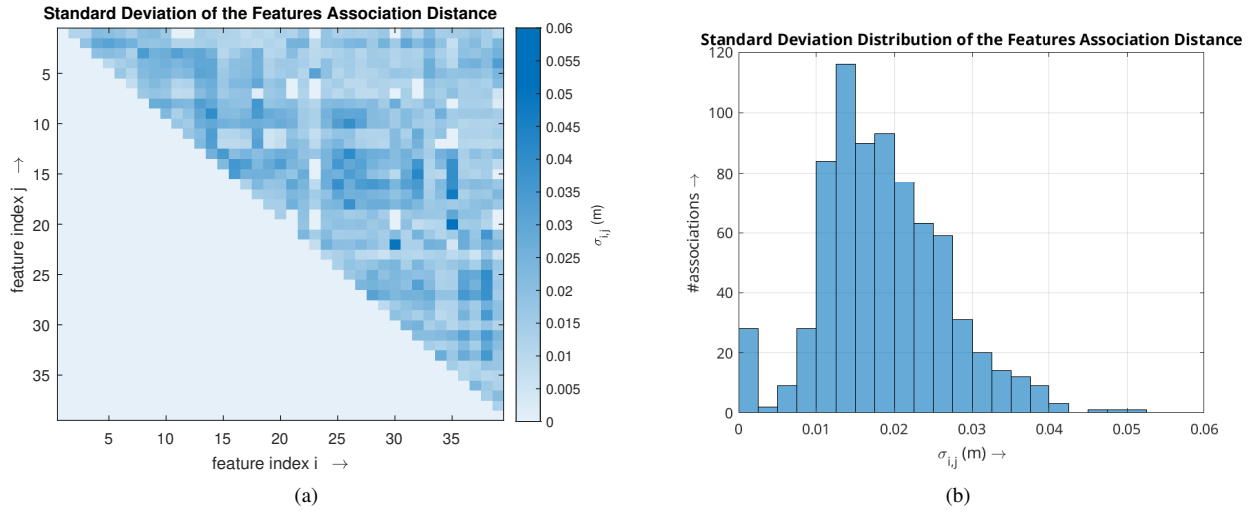


Fig. 5: Standard deviation analysis of the distance between corresponding features: (a) association matrix; (b) histogram distribution.

measures (zero mean and 0.03 m standard deviation according to the specifications of the Hokuyo UST-10LX sensor).

The maximum standard deviation of features association distance obtained in the experiments is 0.051 m. Although this value is greater than the one characteristic of the sensor, most of the associations have a non-zero standard deviation lower or equal to 0.03 m, representing 91.5% of the possible associations between features. Note that only non-zero values must be considered because, due to the sensor not having a 360° FOV and to possible physical obstructions on the laser view, not all associations are physically possible (in this case, 20 associations are not possible). Even when considering associations with a deviation lower or equal to 0.03 m, the proportion remains very significant at 59.3%. Thus, these results on the feature association distance underline the usefulness of the proposed corner-like features detector for localisation processes, given that the geometric relations between features remain consistent and invariant.

## V. CONCLUSIONS

The proposed corner-like feature extraction algorithm achieved in the experiments standard deviations on the relative position between features lower than the sensor noise and visibility ratios higher than 75% in some cases, with very low false positives rates. These results indicate consistency and invariance properties in space of the proposed feature, demonstrating the possible contribution of this work for the localisation and mapping problems on mobile robots. Future work will be performed in integrating the proposed feature detector into a localisation system and further evaluation and comparison to other localisation methodologies.

## REFERENCES

- [1] R.B. Sousa, H.M. Sobreira, and A.P. Moreira. “A systematic literature review on long-term localization and mapping for mobile robots”. In: *Journal of Field Robotics* 40.5 (2023), pp. 1245–1322. DOI: 10.1002/rob.22170.
- [2] R. Siegwart, I.R. Nourbakhsh, and D. Scaramuzza. *Introduction to autonomous mobile robots*. The MIT Press, 2004.
- [3] Giorgio Grisetti, Cyrill Stachniss, and Wolfram Burgard. “Improved Techniques for grid mapping with Rao-Blackwellized particle filters”. In: *IEEE Transactions on Robotics* 23.1 (2007), pp. 34–46. DOI: 10.1109/TRO.2006.889486.
- [4] K.M. Wurm, C. Stachniss, and G. Grisetti. “Bridging the gap between feature- and grid-based SLAM”. In: *Robotics and Autonomous Systems* 58.2 (2010), pp. 140–148. DOI: 10.1016/j.robot.2009.09.009.
- [5] H. Sobreira, A.P. Moreira, P.G. Costa, and J. Lima. “Robust mobile robot localization based on security laser scanner”. In: *2015 IEEE Int. Conf. Autom. Rob. Sys. Compet. (ICARSC)*. 2015, pp. 162–167. DOI: 10.1109/ICARSC.2015.28.
- [6] J.A. Castellanos, J. Neira, O. Strauss, and J.D. Tardos. “Detecting high level features for mobile robot localization”. In: *1996 IEEE/SICE/RSJ Int. Conf. Multisens. Fusion Integr. Intell. Syst. (MFI)*. 1996, pp. 611–618. DOI: 10.1109/MFI.1996.572237.
- [7] S.I. Roumeliotis and G.A. Bekey. “SEGMENTS: a layered, dual-Kalman filter algorithm for indoor feature extraction”. In: *2000 IEEE/RSJ Int. Conf. Intell. Robots Syst. (IROS)*. Vol. 1. 2000, pp. 454–461. DOI: 10.1109/IROS.2000.894646.
- [8] H.A. Mohamed, A.M. Moussa, M.M. Elhabiby, N. El-Sheimy, and A.B. Sesay. “Improved real-time scan matching using corner features”. In: *The International Archives of the Photogrammetry, Remote Sensing and Spatial Information Sciences XLI-B5* (2016), pp. 533–539. DOI: 10.5194/isprs-archives-XLI-B5-533-2016.

- [9] Y. Liu, L. Sui, P. Li, et al. "A radar linear feature fitting algorithm combining adaptive clustering and corner detection operator". In: *Journal of Sensors* 2023 (2023), p. 6991467. DOI: 10.1155/2023/6991467.
- [10] P. Nunez, R. Vazquez-Martin, J.C. del Toro, A. Bandera, and F. Sandoval. "Feature extraction from laser scan data based on curvature estimation for mobile robotics". In: *2006 IEEE Int. Conf. Robot. Autom. (ICRA)*. 2006, pp. 1167–1172. DOI: 10.1109/ROBOT.2006.1641867.
- [11] R. Vázquez-Martín, P. Núñez, A. Bandera, and F. Sandoval. "Curvature-based environment description for robot navigation using laser range sensors". In: *Sensors* 9.8 (2009), pp. 5894–5918. DOI: 10.3390/s90805894.
- [12] X. Feng, S. Guo, X. Li, and Y. He. "Robust mobile robot localization by tracking natural landmarks". In: *Artif. Intell. Comput. Intell. (AICI 2009)*. 2009, pp. 278–287. DOI: 10.1007/978-3-642-05253-8\_31.
- [13] S.T. Pfister, S.I. Roumeliotis, and J.W. Burdick. "Weighted line fitting algorithms for mobile robot map building and efficient data representation". In: *2003 IEEE Int. Conf. Robot. Autom. (ICRA)*. 2003, pp. 1304–1311. DOI: 10.1109/ROBOT.2003.1241772.
- [14] H. Gao, X. Zhang, Y. Fang, and J. Yuan. "International Journal of Advanced Robotic Systems". In: *A line segment extraction algorithm using laser data based on seeded region growing* 15.1 (2018). DOI: 10.1177/1729881418755245.
- [15] Z. Falomir, L. Museros, V. Castelló, and L. Gonzalez-Abril. "Qualitative distances and qualitative image descriptions for representing indoor scenes in robotics". In: *Pattern Recognition Letters* 34.7 (2013), pp. 731–743. DOI: 10.1016/j.patrec.2012.08.012.
- [16] N. Certad, R. Acuna, A. Terrones, D. Ralev, J. Cappelletto, and J.C. Grieco. "Study and improvements in landmarks extraction in 2D range images based on an adaptive curvature estimation". In: *2012 VI Andean Region Int. Conf.* 2012, pp. 95–98. DOI: 10.1109/Andescon.2012.31.
- [17] H.G. Jung, Y.H. Cho, P.J. Yoon, and J. Kim. "Scanning laser radar-based target position designation for parking aid system". In: *IEEE Transactions on Intelligent Transportation Systems* 9.3 (2008), pp. 406–424. DOI: 10.1109/TITS.2008.922980.
- [18] W. Lin, J. Hu, H. Xu, C. Ye, X. Ye, and Z. Li. "Graph-based SLAM in indoor environment using corner feature from laser sensor". In: *2017 32nd Youth Academic Annu. Conf. Chinese Associat. Autom. (YAC)*. 2017, pp. 1211–1216. DOI: 10.1109/YAC.2017.7967597.
- [19] Y. Liu, L. Zhang, K. Qian, et al. "An adaptive threshold line segment feature extraction algorithm for laser radar scanning environments". In: *Electronics* 11.11 (2022), p. 1759. DOI: 10.3390/electronics11111759.
- [20] S. Qu, G. Chen, C. Ye, et al. "An efficient L-shape fitting method for vehicle pose detection with 2D LiDAR". In: *2018 IEEE Int. Conf. Robot. Biomimetics (ROBIO)*. 2018, pp. 1159–1164. DOI: 10.1109/ROBIO.2018.8665265.
- [21] E. Fernández-Moral, J. González-Jiménez, and V. Arévalo. "Extrinsic calibration of 2D laser rangefinders from perpendicular plane observations". In: *International Journal of Robotics Research* 34.11 (2015), pp. 1401–1417. DOI: 10.1177/0278364915580683.
- [22] Y. Zhao, F. Liu, and R. Wang. "Location technology of indoor robot based on laser sensor". In: *2016 IEEE Int. Conf. Softw. Eng. Serv. Sci. (ICSESS)*. 2016, pp. 683–686. DOI: 10.1109/ICSESS.2016.7883160.
- [23] H. Bay, T. Tuytelaars, and L. Van Gool. "SURF: speeded up robust features". In: *Computer Vision – ECCV 2006*. 2006, pp. 404–417. DOI: 10.1007/11744023\_32.
- [24] J.A. Castellanos and J.D. Tardos. "Laser-based segmentation and localization for a mobile robot". In: *Proceedings of the Second World Automation Congress (WAC'96)*. 1996.
- [25] J. Xavier, M. Pacheco, D. Castro, A. Ruano, and U. Nunes. "Fast line, arc/circle and leg detection from laser scan data in a player driver". In: *2005 IEEE Int. Conf. Robot. Autom. (ICRA)*. 2005, pp. 3930–3935. DOI: 10.1109/ROBOT.2005.1570721.
- [26] M.A. Fischler and Robert C. Bolles. "Random sample consensus: a paradigm for model fitting with applications to image analysis and automated cartography". In: *Communications of the ACM* 24.6 (1981), pp. 381–395. DOI: 10.1145/358669.358692.
- [27] L. Muñoz, M. Villanueva, and C.A. Álvarez. "An extended line tracking algorithm". In: *2013 IEEE Int. Autumn Meet. Pow. Elect. Comput. (ROPEC)*. 2013, pp. 1–5. DOI: 10.1109/ROPEC.2013.6702752.
- [28] M. Ester, H.-P. Kriegel, J. Sander, and X. Xu. "A density-based algorithm for discovering clusters in large spatial databases with noise". In: *Proceedings of the Second International Conference on Knowledge Discovery and Data Mining (KDD'96)*. 1996, pp. 226–231.
- [29] G.A. Borges and M.-J. Aldon. "Line extraction in 2D range images for mobile robotics". In: *Journal of Intelligent and Robotic Systems* 40.3 (2004), pp. 267–297. DOI: 10.1023/B:JINT.0000038945.55712.65.
- [30] J.F. Kenney and E.S. Keeping. "Linear regression and correlation". In: 3rd ed. *Mathematics of Statistics*. Princeton: Van Nostrand, 1962. Chap. 15, pp. 252–285.
- [31] R.B. Sousa, M.R. Petry, and A.P. Moreira. "OptiOdom: a generic approach for odometry calibration of wheeled mobile robots". In: *Journal of Intelligent & Robotic Systems* 105 (2022), p. 39. DOI: 10.1007/s10846-022-01630-3.
- [32] S. Macenski and I. Jambrecic. "SLAM toolbox: SLAM for the dynamic world". In: *The Journal of Open Source Software* 6.61 (2021), p. 2783. DOI: 10.21105/joss.02783.
- [33] S. Thrun, W. Burgard, and D. Fox. *Probabilistic robotics*. The MIT Press, 2005.